

# Analysis and validation of a multiple output series resonant converter

Zoran Pavlović; Jesús A. Oliver; Pedro Alou; Óscar Garcia; José A. Cobos

Centro de Electrónica Industrial  
Universidad Politécnica de Madrid  
Madrid, Spain

**Abstract**—In this paper a novel bidirectional multiple port dc/dc transformer topology is presented. The novel concept for dc/dc transformer is based on the Series Resonant Converter (SRC) topology operated at its resonant frequency point. This allows for higher switching frequency to be adopted and enables high efficiency/high power density operation. The feasibility of the proposed concept is verified on a 300W, 700 kHz three port prototype with 390V input voltage and 48V and 12V output voltages. A peak overall efficiency of 93% is measured at full load. A very good load and cross regulation characteristic of the converter is observed in the whole load range, from full load to open circuit. The sensitivity analysis of the resonant capacitance is also performed showing very slight deterioration in the converter performances when a resonant capacitor is changed  $\pm 30\%$  of its nominal value.

## I. INTRODUCTION

The research on high performance bidirectional dc/dc converters is gaining on importance, since they are key components in designing more efficient power distribution systems. In this context, multiple port converters have been attracting increased investigation effort, [1]-[3]. They are widely employed in the hybrid power distribution systems to control power flow between different power sources, storage elements and loads. Multiple port structures are also desirable from the viewpoints of cost, area and control. The power flow is typically controlled using phase shift control scheme, alone or combined with PWM control.

In order to provide power to the electronic loads that demand different supply voltages, multiple output converters can be used. Several approaches have been proposed to deliver independently and tightly regulated output voltages, [4]-[6]. Pulsewidth and complementary pulsewidth PFM modulation are used in [4] to control the output voltages. In [5] the main output voltage is controlled by the switching frequency modulation while in [6] the outputs are regulated by the phase shifting between the independent leading legs and the shared lagging leg. Besides the complex control, the solutions presented in [4] and [6] use one transformer per output and inductances to filter the output voltages, what limits converter power density.

In typical power distribution architectures the power is delivered to the load through multiple voltage buses, [7]. The

connection of each of those buses to the common input voltage is done using single-input single-output dc/dc converters. The performances of those single-input single-output dc/dc converters are key issues to determine the performances of the whole power distribution architecture. Integration of different voltage buses into a single power node leads to a reduction of the required multiple converter stages used in the conventional architectures.

This paper is aimed at integrating different converter stages, typically found in power delivery architectures, into a novel bidirectional multiple port power node to overcome the aforementioned drawbacks. The new power node topology is based on a resonant converter topology and reduces to only one the number of magnetic components. Soft switching commutations make possible high switching frequencies to be adopted and high power densities to be achieved. Possible problems regarding stray inductances are eliminated since they are absorbed into the circuit elements. The converter features very good inherent load and cross regulation due to the small output impedances. However, the input voltage regulation capability is lost since the converter is operated at its resonant frequency with 50% duty cycle. Unlike the conventional architectures where each single-input single-output dc/dc converter has its own control, the power node control is relocated and centralized to the previous stage to regulate the input voltage of the power node.

## II. THE PROPOSED MULTIPLE PORT DC/DC TRANSFORMER

The proposed bidirectional multiple port dc/dc transformer is based on the series resonant converter topology, [8]-[10]. The extension of the SRC converter to the multiple output topology is achieved by adding transformer windings and the corresponding inverter/rectifier cells. An example of a three port dc/dc transformer is shown in Figure 1. It consists of a half bridge inverter on the primary side and two full bridge rectifiers on the secondary side of the high frequency transformer, that provides isolation and is framed with dashed line in Figure 1. For each port, the designer can select either a full bridge or a half bridge type inverter/rectifier to permit bidirectional power flow and optimize the converter operation. One of the key benefits of this multiple port converter is that the transformer is the only magnetic component in the design and its leakage inductances form part of the resonant tank

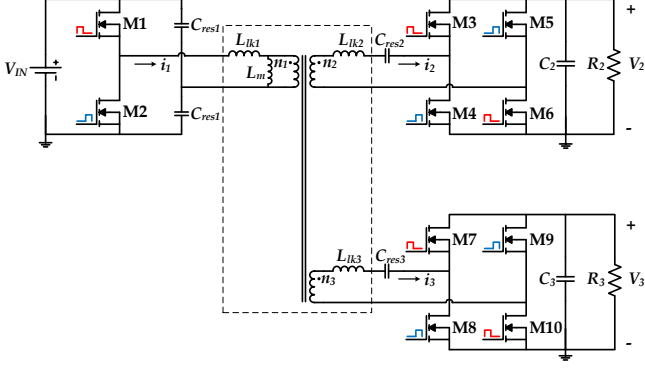


Figure 1. Three port SRC based bidirectional dc/dc transformer.

networks on both the input and the output ports. No additional inductor is required for output voltage filtering. Another advantage is that the converter is operated at fixed switching frequency with complementary and constant duty cycle (approximately 50%) switch driving signals (red and blue gate signals ( $v_{GS}$ ) in Figure 2).

The switches on the opposite diagonals in the inverter cells are driven simultaneously, as it is indicated in Figure 1 with red and blue gate signals. A resonant tank at each port is comprised of the corresponding leakage inductance and a series capacitor; if the selected inverter/rectifier is the half bridge, the resonant capacitance is just provided by the half bridge capacitors themselves, i.e., the series capacitance seen by resonant inductor is the equivalent parallel connection of the half bridge capacitors. When the full bridge inverter/rectifier is used, the series capacitor is placed between the transformer and the full bridge cell. The resonant frequencies of all three resonant tank networks are tuned to the switching frequency. Reordering the well-known relation given in (1) between the tank resonant frequency,  $f_{sw}$ , and its inductance,  $L$ , and capacitance,  $C$ , the expression for the selection of the resonant capacitors  $C_{res1}$ ,  $C_{res2}$  and  $C_{res3}$  is given in (2), where  $i \in [1,2,3]$  and  $j=0$  for full bridge and  $j=1$  for half bridge inverter:

$$f_{sw} = \frac{1}{2\pi\sqrt{LC}} \quad (1)$$

$$C_{res,i} = \frac{1}{(2\pi f_{sw})^2 2^j L_{lk,i}} \quad (2)$$

### A. Operating principle

Basic voltage and current waveforms of the three port dc/dc transformer when the magnetizing current is taken into account are shown in Figure 2. Due to the magnetizing current effect, the resonant tank currents have some non-zero values at the ends of each half cycle. Four operating stages can be distinguished, according to the conduction state of the switches and the magnetizing current direction.

**Stage 1** [ $t_0 - t_1$ ]: At time  $t_0$  the switches M1, M3, M6, M7 and M10 are turned on and positive voltages  $V_{IN}/2$ ,  $V_2$  and  $V_3$  are applied to the transformer primary and secondary resonant tanks. These voltages are ideally proportional to the

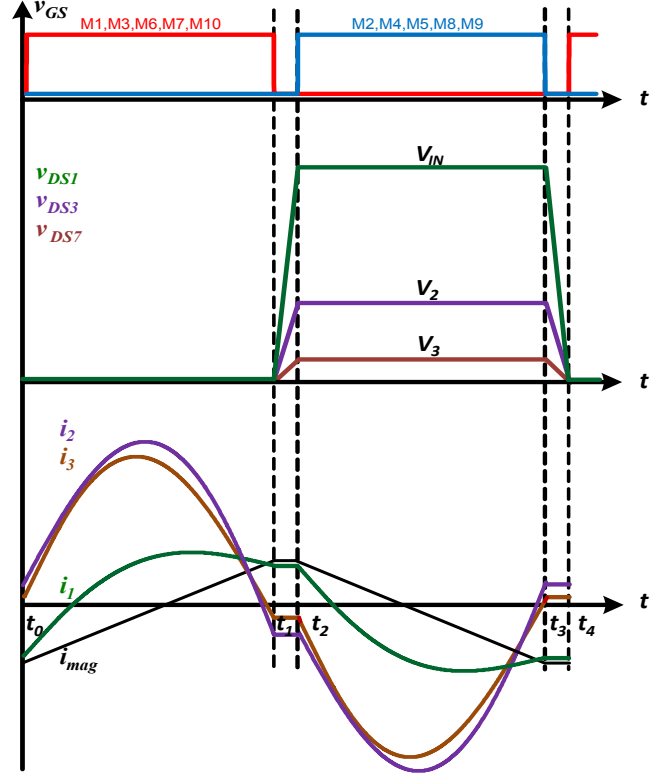


Figure 2. Voltage and current waveforms of the three port dc/dc transformer from Figure 1.

transformer turns ratio  $n_0.n_1.n_2$ . The slight difference between them is due to the voltage drops on the transformer and switch resistances on the current path. The higher these resistances are, the higher are the voltage drops and the differences of the output voltages,  $V_2$  and  $V_3$ , from their nominal values. The switches M3, M6, M7 and M10 are turned off with nearly ZCS at time  $t_1$  when the positive sinusoidal currents  $i_1$  and  $i_2$  cross zero, while the switch M1 is turned off with the peak magnetizing current.

**Stage 2** [ $t_1 - t_2$ ]: During this stage the voltage across the series resonant capacitors can be considered constant since these capacitances are much higher than the parasitic capacitances. It can also be assumed that the magnetizing current is approximately constant during the dead time interval. At  $t_1$  the positive peak magnetizing current is distributed among the primary and both secondary side tanks and discharges the capacitances  $2C_{oss1}$ , a parallel connection of the switches' M1 and M2 parasitic drain-source capacitances,  $C_{oss2}$ ,  $C_{oss3}$  and  $C_p$ , which represents the equivalent parasitic transformer winding capacitance seen from the primary side. At time  $t_2$  parasitic drain-source capacitances of the switches M1, M3, M6, M7 and M10 are charged to their respective voltages and the switches M2, M4, M5, M8 and M9 are discharged to be turned on with ZVS. Also, due to the redistribution of the magnetizing current between the primary and secondary sides, the switches M4, M5, M8 and M9 are turned on with small negative portion of the magnetizing current (Figure 2).

**Stage 3** [ $t_2 - t_3$ ]: In the time interval  $t_2 - t_3$  a similar circuit operation as in the time interval  $t_0 - t_1$  can be observed. Since all the switches are turned on with ZVS and turned off with

nearly ZCS, a significant reduction in switching losses is achieved. This permits selection of high switching frequency to reduce the size of the transformer and obtain high power density.

*Stage 4* [ $t_3 - t_4$ ]: In this stage the negative peak magnetizing current charges parasitic drain-source capacitances,  $C_{oss}$ , of the switches M2, M4, M5, M8 and M9, discharges  $C_{oss}$  of M1, M3, M6, M7 and M10 and also charges parasitic self-capacitance of the transformer windings,  $C_p$ . The time interval  $t_3 - t_4$  completes one switching cycle.

Unlike the single output dc/dc transformer based on SRC where only one resonant capacitor is needed to resonate with the transformer primary and secondary side leakage inductances, in case of three port dc/dc transformer three resonant capacitors are needed. Let's assume that only two resonant capacitors are selected according to (2) and the third one is omitted. If the current waveforms on the transformer sides with added resonant capacitors were sinusoidal with ZCS, there would be a voltage drop across the inductor on the side with no added capacitor and its current would be a cosine function. On the other hand, the current through the single inductor has to be sinusoidal due to the transformer current relation. Therefore, a different current distribution in the transformer windings would be established, leading to a loss of ZCS condition at turn off in all the switches and, as a consequence, switching losses would be higher. Therefore, the impact of the transformer leakage inductances at each winding has to be canceled at the switching frequency.

### B. Self and cross load regulation

Another advantage of the proposed multiple port converter is a good load regulation and cross-regulation among the outputs due to its inherent low output impedances. Load variation at one output port has very small effect on its own output voltage and on the others. In order to calculate its output resistances, an equivalent circuit of the three port dc/dc transformer seen from the primary side when the power transfer occurs is shown in Figure 3. The square voltage sources, that represent the output voltage of the half bridge inverter and input voltages of the full bridge rectifiers seen from the primary side, are in phase and their values are given in Figure 3. Since all the three resonant tanks are tuned to the switching frequency, the resonant tank currents  $i_1$ ,  $i_2$  and  $i_3$  will contain only fundamental frequency components. It can be assumed that the currents in phase with the square voltage sources are given as in (3):

$$i_{k,ph} = I_{m,k} \sin \omega t \quad (3)$$

where  $k \in [2,3]$ ,  $\omega = 2\pi f_{sw}$  and the amplitudes  $I_{m,k}$  depend on the output currents  $I_{OUT,k}$ , which are the average values of the rectified resonant tank currents:

$$I_{m,k} = \frac{\pi}{2} I_{OUT,k} \quad (4)$$

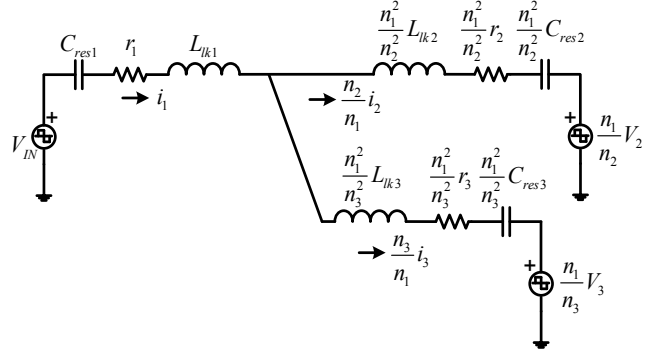


Figure 3. Equivalent circuit of the three port dc/dc transformer seen from the primary side.

By converting the sinusoidal voltage drops on the current path parasitic resistances  $r_1$ ,  $r_2$  and  $r_3$  into square voltages, the expressions needed to calculate the output voltages are given by:

$$\frac{V_{IN}}{2} - \frac{\pi}{4} r_1 \left( \frac{n_2}{n_1} I_{m,2} + \frac{n_3}{n_1} I_{m,3} \right) - \frac{\pi}{4} \frac{n_1^2}{n_2^2} r_2 \frac{n_2}{n_1} I_{m,2} - \frac{n_1}{n_2} V_2 = 0 \quad (5)$$

$$\frac{V_{IN}}{2} - \frac{\pi}{4} r_1 \left( \frac{n_2}{n_1} I_{m,2} + \frac{n_3}{n_1} I_{m,3} \right) - \frac{\pi}{4} \frac{n_1^2}{n_3^2} r_3 \frac{n_3}{n_1} I_{m,3} - \frac{n_1}{n_3} V_3 = 0 \quad (6)$$

where  $r_1, r_2$  and  $r_3$  are comprised of the switch on resistances, layout and the transformer equivalent series resistance in the primary and the secondary sides circuits. After the rearrangement of the expressions (5) and (6) the output voltages are expressed by the self and mutual output resistances as:

$$V_2 = \frac{n_2}{n_1} \frac{V_{IN}}{2} - \frac{\pi^2}{8} \left( \frac{n_2^2}{n_1^2} r_1 + r_2 \right) I_{OUT,2} - \frac{\pi^2}{8} \frac{n_2 n_3}{n_1^2} r_1 I_{OUT,3} \quad (7)$$

$$V_3 = \frac{n_3}{n_1} \frac{V_{IN}}{2} - \frac{\pi^2}{8} \frac{n_3 n_2}{n_1^2} r_1 I_{OUT,2} - \frac{\pi^2}{8} \left( \frac{n_3^2}{n_1^2} r_1 + r_3 \right) I_{OUT,3} \quad (8)$$

The inherent load regulation is given by those resistances that depend on the MOSFETs on-resistances, layout and transformer series resistances and can have very small values. Therefore, the output voltage deviations from their nominal values will not be significant. Besides, as the output currents decrease, the resonant tank currents also decrease making possible low losses and high efficiency operation at light load conditions to be obtained.

### III. EXPERIMENTAL VERIFICATION

The performance of the proposed three port dc/dc transformer are analyzed on a prototype with 390V input voltage,  $V_{IN}$ , and 48V/5A,  $V_2$ , and 12V/5A,  $V_3$ , outputs. The selected switching frequency is  $f_{sw} = 700$  kHz. The switches used on the primary side are IPD50R520CP (550V, 0.52Ω, 13nC) and on the secondary side IRFH5406PbF (60V, 14.4mΩ, 21nC) and IRF6631 (30V, 6mΩ, 12nC). The input

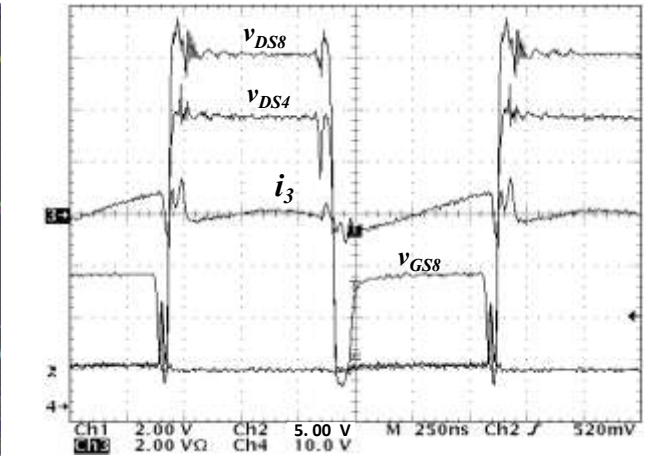
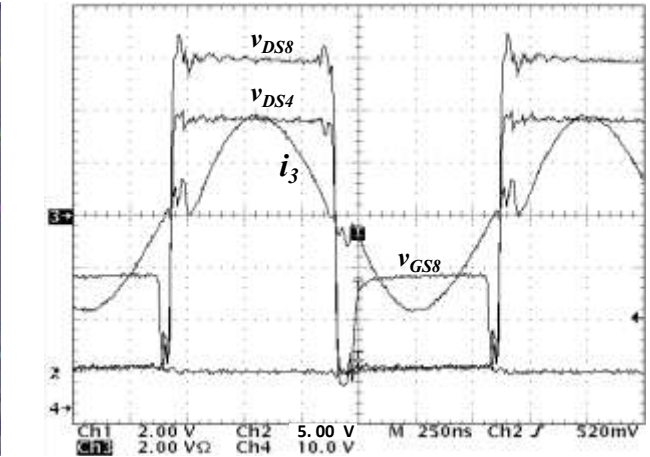
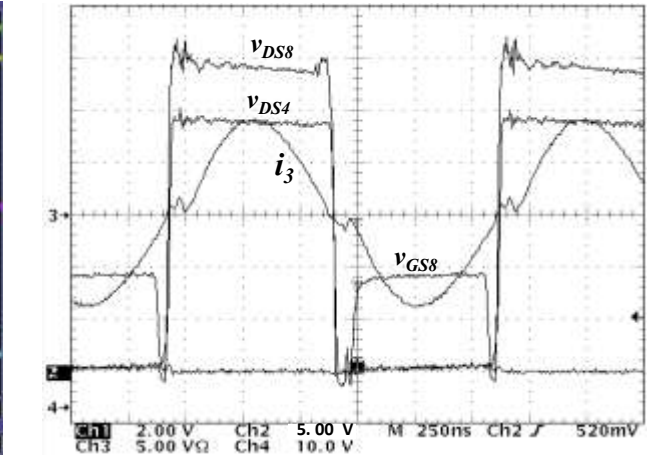
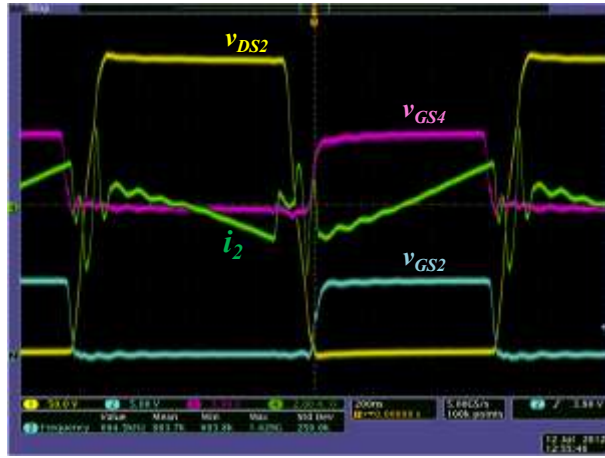
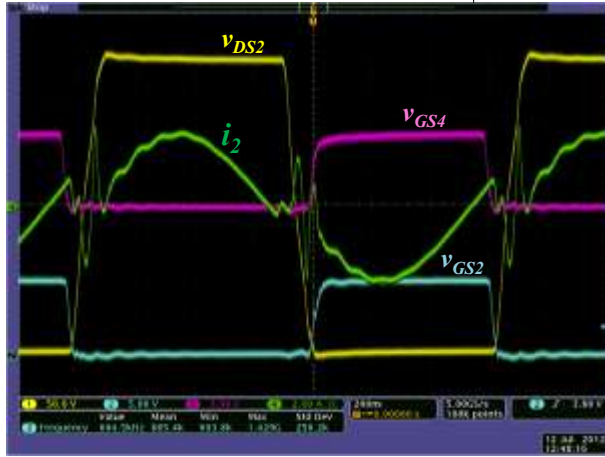
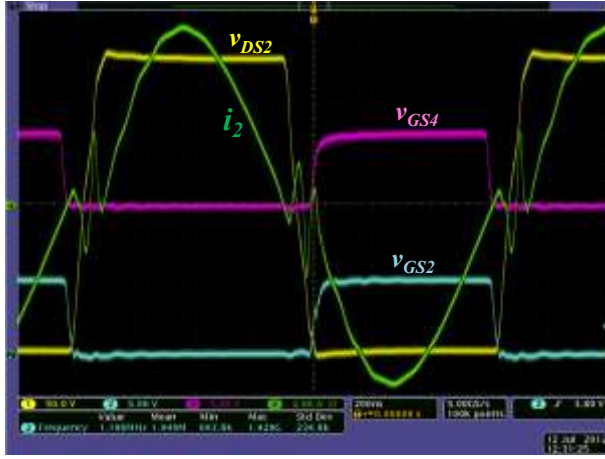


Figure 4. Experimental waveforms of the three port dc/dc transformer for the same loading conditions at both outputs: (a) full load, (b) 40% of the load and (c) no load condition. The voltage scale for the waveform  $v_{DS2}$  is  $50V/div$  and for  $v_{GS2}$  and  $v_{GS4}$  is  $5V/div$ . The current scale for  $i_2$  is  $2A/div$ .

and output filter capacitor values are  $C_{IN}=1.5\mu F$ ,  $C_2=12\mu F$  and  $C_3=12\mu F$ . The adjusted and measured resonant capacitor values are  $C_{res1\_high\ side}=560nF$ ,  $C_{res1\_low\ side}=550nF$ ,  $C_{res2}=1.8\mu F$  and  $C_{res3}=2.6\mu F$ . Since the total parasitic inductances  $L_{lk1}$ ,  $L_{lk2}$  and  $L_{lk3}$  on current paths were not known with certainty the following procedure was used to determine the resonant capacitor values. The resonant capacitors  $C_{res1}$

were selected according to their theoretical predictions. The currents  $i_2$  and  $i_3$  were measured at full load and the resonant capacitors  $C_{res2}$  and  $C_{res3}$  were adjusted until the ZCS conditions at both outputs were achieved. It was then possible to calculate the total parasitic inductances on the current paths in the primary and the secondary side circuits using the equation (1):  $L_{lk1}=33nH$ ,  $L_{lk2}=20nH$  and  $L_{lk3}=14nH$ .

One planar EE core (E18/4/10R-3F3) was used to build the transformer with two parallel windings and a turns ratio of  $n_1:n_2:n_3=16:4:1$  achieving a transformer power density of  $3.2\text{kW/in}^3$ . A gap ( $560\mu\text{m}$ ) is adjusted to obtain the magnetizing inductance of  $L_m=24\mu\text{H}$  needed to obtain ZVS transitions in all the switches. The total self-capacitance of the planar windings seen on the primary side is measured to be  $C_p=240\text{pF}$  which is much higher than the  $C_{oss, tr}=63\text{pF}$  of the equivalent output capacitance of one primary side switch. Figure 5 shows the cross section of the realized transformer.

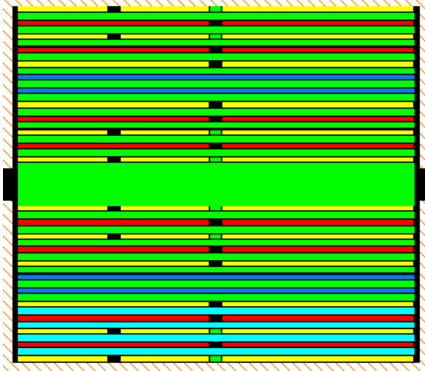


Figure 5. Cross section of the EE18/4/10R-3F3 planar transformer with two parallel 12 layer  $70\mu\text{m}$  copper PCBs

The experimental waveforms for the steady state operation of the three port dc/dc transformer are shown in Figure 6 for both outputs are operating at full load, 40% of the load and no load conditions. In all three cases all the switches operate under ZVS condition which is not dependent on the load. At full load condition the switches in both full bridge rectifiers turn off with ZCS. A high frequency current ringing between parasitic capacitors and the leakage inductances can also be observed in the dead time interval in all  $i_2$  current waveforms. It can also be noticed comparing Figure 6(a) and Figure 6(b) that  $i_2$  current waveform changes as the load changes. This is due to the effect of the magnetizing current. Namely, when the magnetizing current is very small the resonant tank currents are sinusoidal, as well as the voltage drops across the resonant tanks, and remain sinusoidal for each load combination at the output. When the magnetizing current is not negligible a non-sinusoidal voltage drop across the primary side resonant tank will occur and that will alter the current distribution in the resonant tanks as it can be seen in Figure 6(b). The effect of the magnetizing current is more pronounced at light load since the output currents are lower. At no load condition, Figure 6(c), the magnetizing current is distributed among the tank currents  $i_1$ ,  $i_2$  and  $i_3$ . By placing higher capacitors  $C_{res2}$  and  $C_{res3}$  than the ones calculated in (2) the currents  $i_2$  and  $i_3$  can approach sinusoidal shape at full load. When the load decreases, the ZCS condition in switches M3, M4, M5, and M6 can be recovered at some extent by increasing their on resistances.

The results of the efficiency measurements are shown in Figure 7(a) in the cases when  $V_{IN}=389\text{V}$  and both outputs are changing equally from 10% of the load to full load. The maximum efficiency of 93% is measured at full load. The steady state voltage regulation performances are shown in Figure 7(b) under the same operating condition as in the case

of the efficiency measurement. A very good load regulation characteristic of the converter is observed due to its inherent low output impedances. For light load to full load variation in each output the voltage  $V_2$  variations are kept below 2.5% and in the range of -2.1% to 2.9% for the voltage  $V_3$ .

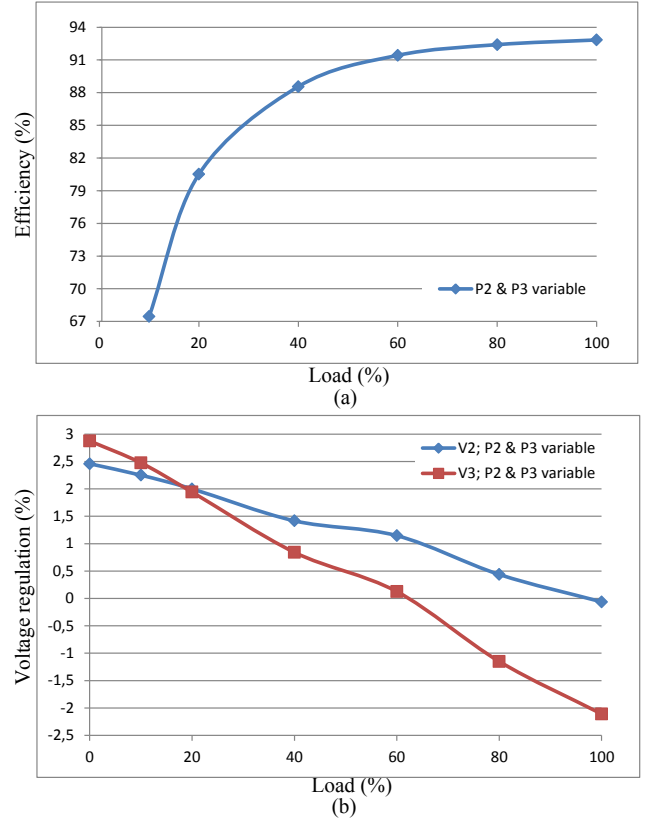


Figure 6. (a) Efficiency measurement of the three port dc/dc transformer when both output are loaded from 10% to 100% of their respective nominal loads and (b) the steady state output voltage regulation for constant input voltage.

#### A. Bidirectional operation

The bidirectional performances of the converter have also been tested from full load to open circuit. In case when the voltage  $V_2$  acts as a power source the results are shown in Figure 8. All the measurements were conducted at  $V_2=50.1\text{V}$ . The measured efficiency figures are similar to those ones measured when the voltage  $V_1$  acted as a power source with approximately 1.5% lower values. Once again, very good load regulation characteristics are observed. The voltage  $V_{IN}$  is maintained within the range of -0.7% to 1.2% when its load varies 100% and the  $V_3$  voltage load is maximal and in the range of -0.7% to 0% when its load is maximal and  $V_3$  voltage load varies 100%. Under the same operating conditions, the  $V_3$  voltage is within the range of -1.1% to 0.5% in the first case and is maintained in the range of -0.9% to 3.4% in the second.

#### IV. TOLERANCE ANALYSIS

In order to check the performance of the proposed converter under parameter variations that affects the resonant frequency and may alter the ZVS-ZCS operation, a tolerance

analysis of the resonant capacitor has been done. In this analysis, the duty cycle or switching frequency have been changed in order to reestablish ZCS condition.

The converter can operate properly even if the resonant capacitors are not precisely tuned to the switching frequency. In this case the switching frequency should be selected as the lower resonant frequency of the two output resonant tanks. If the duty cycle is maintained at approximately 50% as it was before the changes in resonant capacitances, a ZCS condition at the output with higher resonant frequency will be lost. The ZCS condition can be reestablished by changing the duty cycle of the driving signals at the output with higher resonant frequency in the manner that when the resonant tank current half cycle oscillation is finished the switches are turned off. In this way the rms resonant tank current value is also decreased leading to lower conduction losses. Therefore, all the rectifier switches are turned off when their corresponding currents cross zero. The primary side inverter switches are turned off together with the switches at the output with lower resonant frequency. Turn on instants of the switches M1,M3,M6,M7,M10 and M2,M4,M5,M8,M9 can be determined by sensing high and low levels of the drain-source voltage of the switch M2, respectively.

The open loop experimental waveforms that illustrate this are shown in Figure 9 in case when the resonant capacitor  $C_{res2}$  is changed to 70% of its nominal value, ( $C_{res2,nom} = 1.8\mu\text{F}$ ). When the output  $V_2$  is changed from no load to full load and the output  $V_3$  is fully loaded the efficiency drop of at most 1.4% comparing to the nominal case is measured without any other changes in the circuit. On the other hand, when the duty cycle is changed as in Figure 9(b) the efficiency gain of at most +0.9% is observed comparing to the efficiency measurements when only  $C_{res2}$  is changed. However, the voltage  $V_2$  regulation is worsening by approximately 1% in its entire load range. The voltage  $V_3$  regulation characteristic is almost not affected by the change in the duty cycle.

When the resonant capacitor  $C_{res2}$  is changed to 138% of its nominal value the switching frequency has to be changed to 600 kHz as well as the duty cycle of the driving signals of the switches M7, M8, M9 and M10, Figure 10. When the output  $V_2$  is changed from no load to full load and the output  $V_3$  is fully loaded the efficiency loss of at most -1.1% is observed comparing to the nominal case without any other changes in the circuit. When the duty cycle and frequency are changed, the efficiency loss of at most -0.5% is observed comparing to the efficiency measurements when only  $C_{res2}$  is changed. For light load to full load variation at  $V_2$  output, its regulation characteristics is slightly deteriorated after the frequency and duty cycle are changed while the voltage  $V_3$  regulation characteristics is almost not affected. A photo of the prototype is shown in Figure 11.

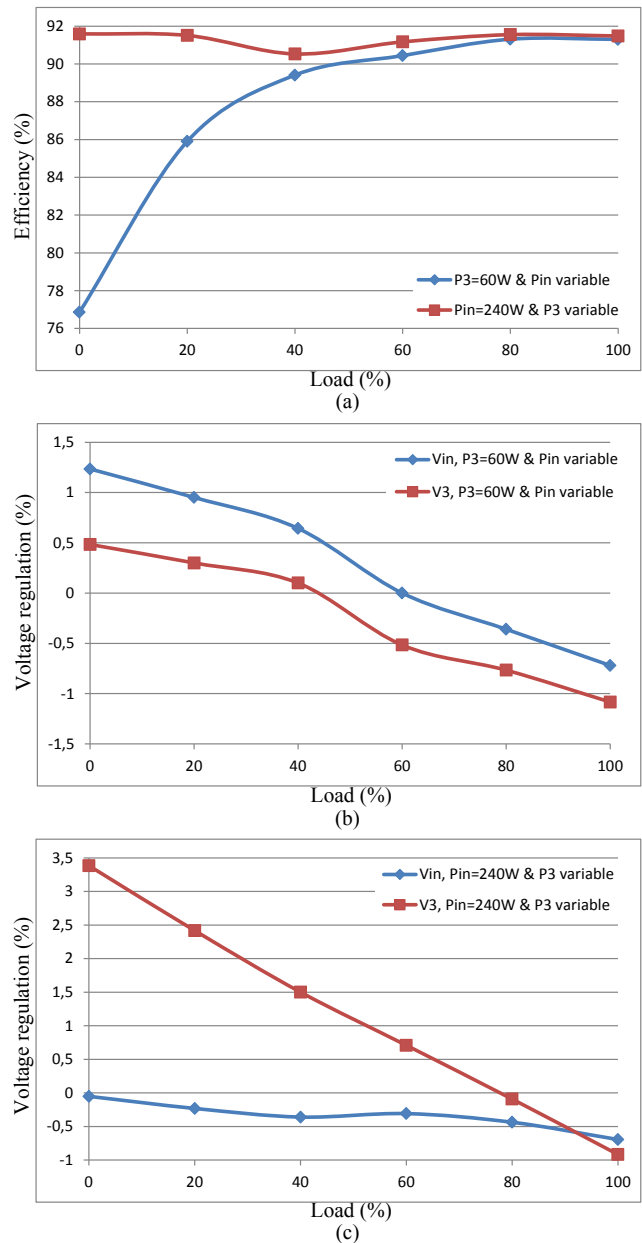
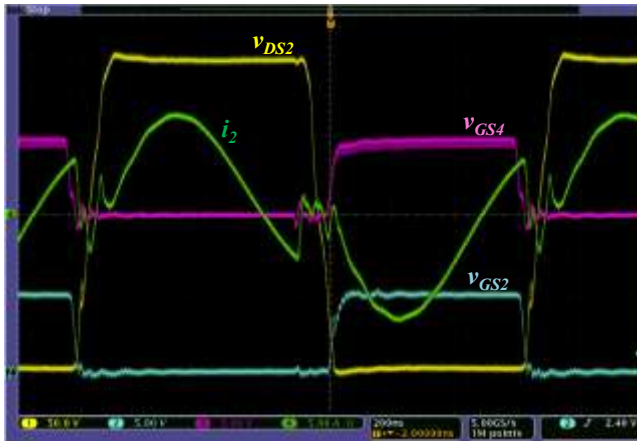
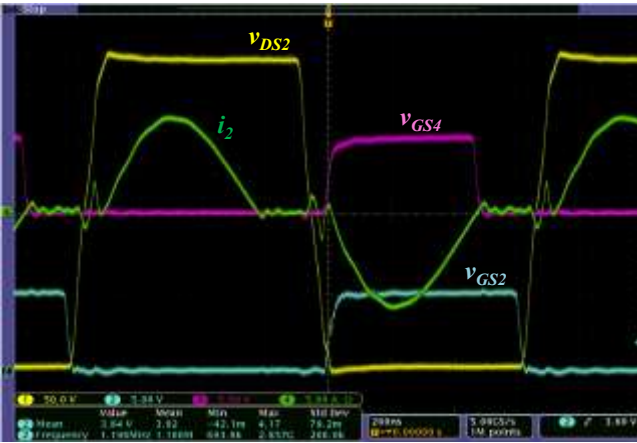


Figure 7. Bidirectional operation of the three port dc/dc transformer when  $V_2$  acts as an input source, one output is fully loaded and the other is swept from no load to full load: (a) efficiency and (b), (c) voltage regulation characteristics.



(a)

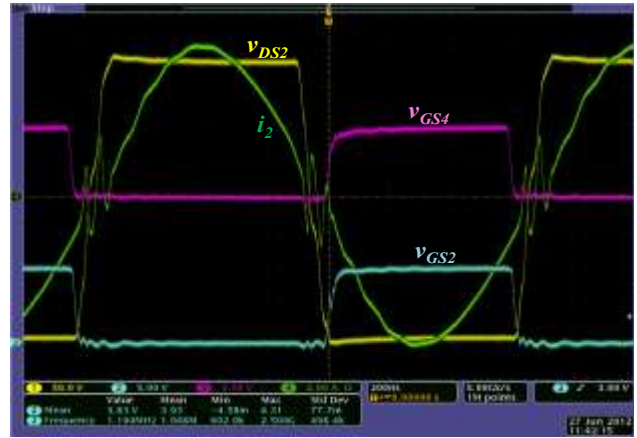


(b)

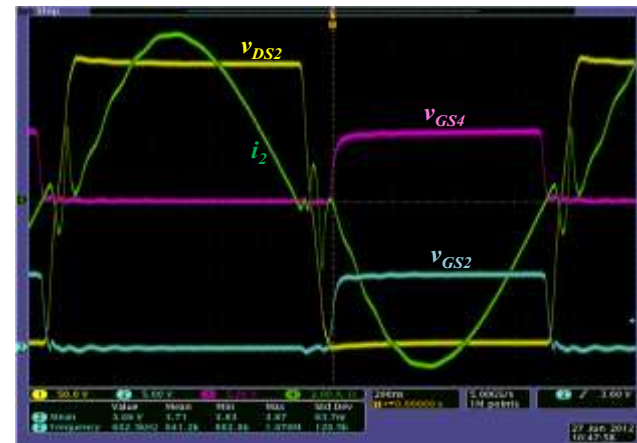
Figure 8. Experimental waveforms when  $C_{res2}$  is decreased 70% of its nominal value: (a) without any change in the switching frequency or driving signals and (b) with adjusted the duty cycle of the driving signals of the switches M3, M4, M5, M6. The voltage scale for  $v_{DS2}$  is 50V/div and for  $v_{GS2}$  and  $v_{GS4}$  is 5V/div. The current scale for  $i_2$  is 5A/div.

## V. CONCLUSIONS

In this paper, a novel multiple port dc/dc bidirectional transformer concept is proposed. The concept is based on the SRC topology operating just at the resonance frequency. In this way, the input voltage regulation capability is lost but high power density operation at constant switching frequency is possible. The converter features the virtual elimination of the power transistor switching losses in all the inverter bridges; ZVS and nearly ZCS are achieved in all the switches. This allows for higher switching frequencies to be adopted and, consequently, reduce the size of the high frequency transformer, which is the only magnetic component in the converter. Full bridge and half bridge inverter/rectifier cell combinations are possible depending on the specifications. A very good load regulation characteristic of the converter is observed due to its inherent low output impedances. The converter performances are experimentally verified on a 300W, 700 kHz prototype with 390V input voltage and 48V and 12V output voltages. The transformer is built on one EE18 core and its power density is 3.2kW/in<sup>3</sup>. The maximum efficiency of 93% is measured at full load. The bidirectional operation is validated from no load to full load with similar



(a)



(b)

Figure 9. Experimental waveforms when  $C_{res2}$  is increased 138% of its nominal value: (a) without any change in the switching frequency or driving signals and (b) with adjusted the switching frequency (to 600kHz) and the duty cycle of the driving signals of the switches M7, M8, M9, M10. The voltage scale for  $v_{DS2}$  is 50V/div and for  $v_{GS2}$  and  $v_{GS4}$  is 5V/div. The current scale for  $i_2$  is 2A/div.



Figure 10. Photo of the three port bidirectional 300W 700 kHz prototype.

performance. The tolerance analysis has shown that the variation of the resonant capacitor  $C_{res2}$  in the range of 70% to 138% of its nominal value causes small efficiency drop and very small deterioration of the voltage regulation characteristics, despite the fact that the switching frequency is not adapted to the resonance frequency variation. If it is necessary, the resonant capacitors' tolerances could be compensated by precise selection of the switching frequency and duty cycle in a closed loop operation.

## REFERENCES

- [1] H. Tao, A. Kotsopoulos, J. L. Duarte, M. A. M. Hendrix, "Constant Switching Frequency Series Resonant Three-port Bi-directional DC-DC Converter," *IEEE Transactions on Power Electronics*, vol. 23, no. 2, March 2008.
- [2] H. Krishnaswami, N. Mohan, "Three-Port Series-Resonant DC-DC Converter to Interface Renewable Energy Sources With Bidirectional Load and Energy Storage Ports," *IEEE Transactions on Power Electronics*, vol. 24, no. 10, October 2009.
- [3] Z. Qian, O. Abdel-Rahman, I. Batarseh, "An Integrated Four-Port DC/DC Converter for Renewable Energy Applications," *IEEE Transactions on Power Electronics*, vol.25, no.7, July 2010.
- [4] Y. Chen and Y. Kang, "A Fully Regulated Dual-Output DC-DC Converter With Special-Connected Two Transformers (SCTTs) Cell and Complementary Pulsewidth Modulation-PFM (CPWM-PFM) ," *IEEE Transactions on Power Electronics*, vol. 25, no. 5, May 2010.
- [5] S. H. Cho, C.-S. Kim and S.-K. Han, "High-Efficiency and Low-Cost Tightly Regulated Dual-Output LLC Resonant Converter," *IEEE Transactions on Industrial Electronics*, vol. 59, no. 7, July 2012.
- [6] Y. Chen, Y. Kang, S. Nie and X. Pei, "The Multiple-Output DC-DC Converter With Shared ZCS Lagging Leg," *IEEE Transactions on Power Electronics*, vol. 26, no. 8, August 2011.
- [7] Dianbo Fu; Bing Lu; Lee, F.C., "1MHz High Efficiency LLC Resonant Converters with Synchronous Rectifier," *IEEE Power Electronics Specialists Conference, 2007*, Page(s): 2404 – 2410.
- [8] I. O. Lee, and G. W. Moon, "Analysis and Design of a Three-Level LLC Series Resonant Converter for High- and Wide-Input Voltage Applications," *IEEE Transactions on Power Electronics*, vol. 27, no. 6, June 2012.
- [9] X. Li, and A. K. S. Bhat, "Analysis and Design of High-Frequency Isolated Dual-Bridge Series Resonant DC/DC Converter," *IEEE Transactions on Power Electronics*, 2010, pp. 850 - 862.
- [10] R. Yu, G. K. Y. Ho, B. M. H. Pong, B. W. K. Ling and J. Lam, "Computer-Aided Design and Optimization of High-Efficiency LLC Series Resonant Converter," *IEEE Transactions on Power Electronics*, vol. 27, no. 7, July 2012.